La maîtrise des vibrations dans les constructions civiles et les structures de précision

André Preumont
Laboratoire des Structures Actives
Université Libre de Bruxelles

AVE 2016
Blois

ULB

1

Tacoma bridge flutter instabilty (1940)
[Wind speed: 40 mph]

Instability resulting from the interaction between the deck vibrations and the unsteady aerodynamic forces acting on the deck

ULB

2

Tacoma bridge Flutter
Computer simulation

ULB

Pedestrian-induced vibrations of bridges

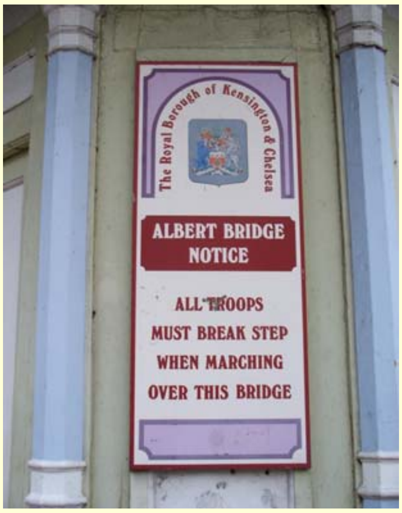

ULB

Pedestrian-induced vibrations of footbridges

Human Activity	Frequency Range (Hz)
Walking	1,6-2,4
Running	2,0-3,5
Jumping	1,8-3,4

Seriate footbridge:
8 walking pedestrians: 1.8 m/s²
4 joggers: 4 m/s²

5

Millenium Bridge London
Pedestrian induced vibration on the opening day
(**synchronization**)

ULB

6

Synchronization of metronomes
[Synchronization of pendulum clocks was first observed by Huygens (17^e)]

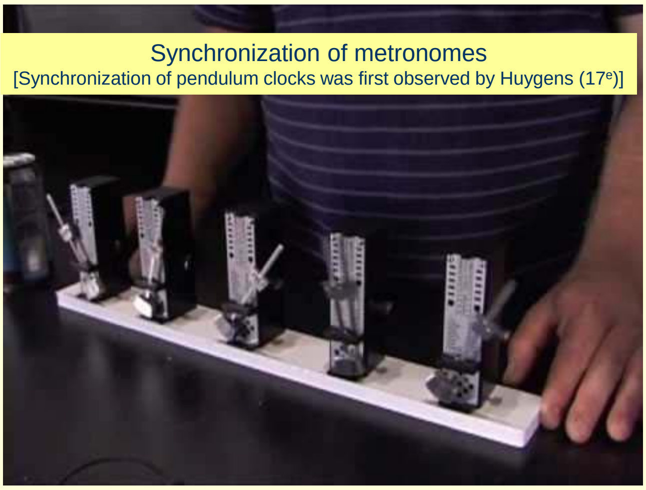

ULB

7

Tallest buildings in the world

ULB

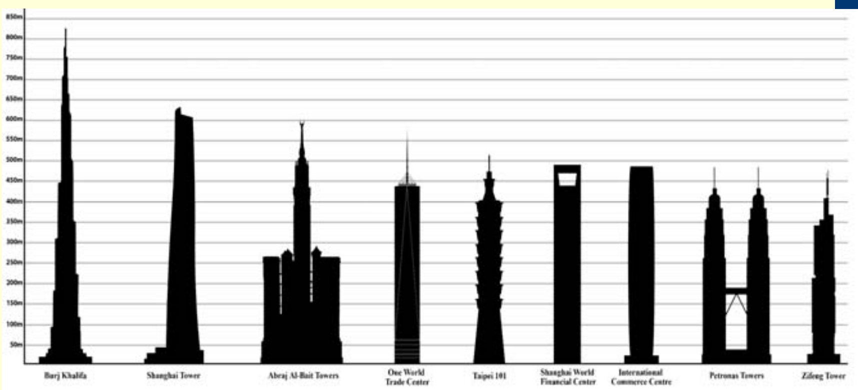

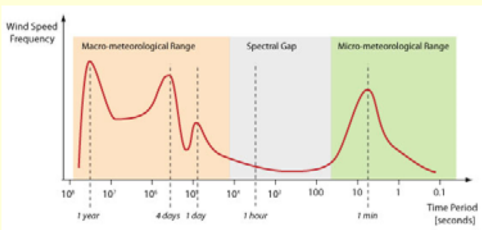

$T_1 \sim 0.1\ n$

8

Reduction of resonance peaks with passive devices:
Tuned Mass Damper (TMD) Dynamic Vibration Absorber (DVA)

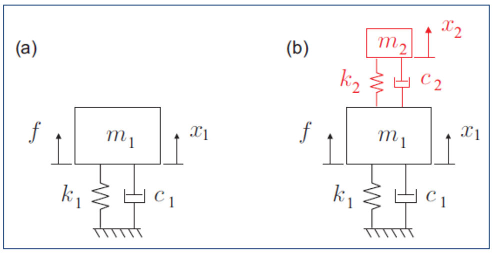

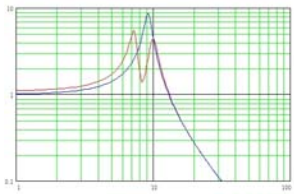

Den Hartog optimum design

$$\frac{\omega_2}{\omega_1} = \frac{1}{1+\mu}$$

$$\xi_2 = \sqrt{\frac{3\mu}{8(1+\mu)}}$$

ULB

9

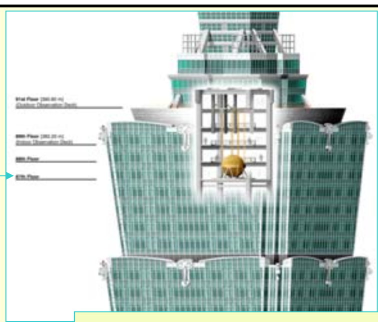

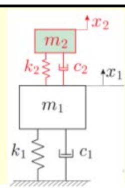

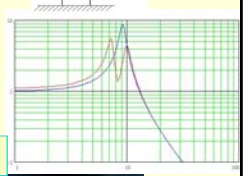

ULB

$T_1 \sim 0.1\, n$

10

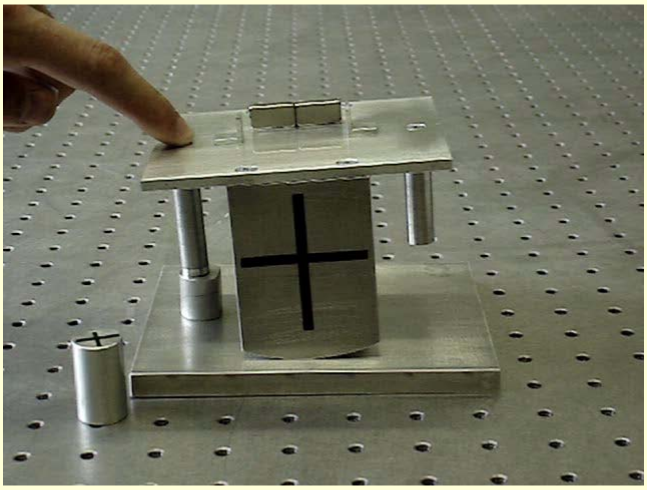

ULB

11

ULB

Active Mass Damper

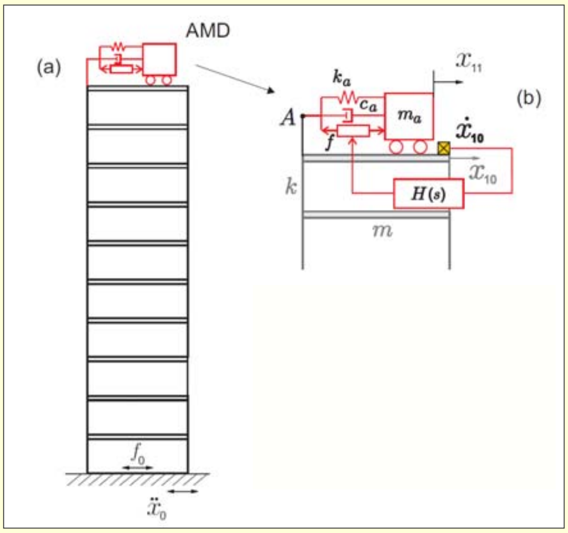

12

Active Mass Damper

Yokohama Landmark Tower
(296 m, 1993)

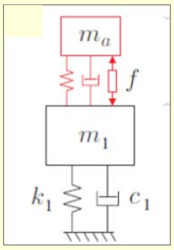

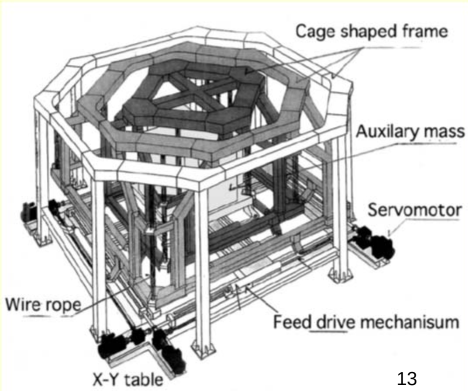

ULB

13

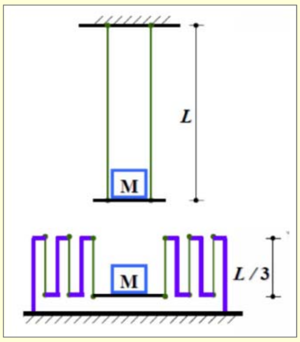

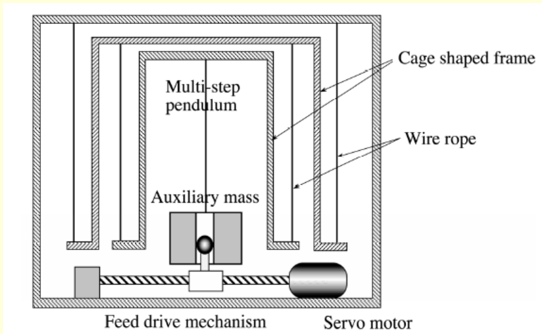

Fig. 2.7 Multi-step pendulum type HMD

(from K. Seto)

ULB

14

ULB

Roller guide HMD

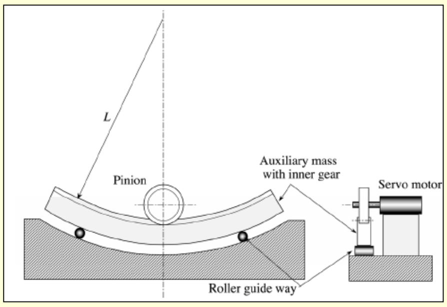

V-shaped HMD

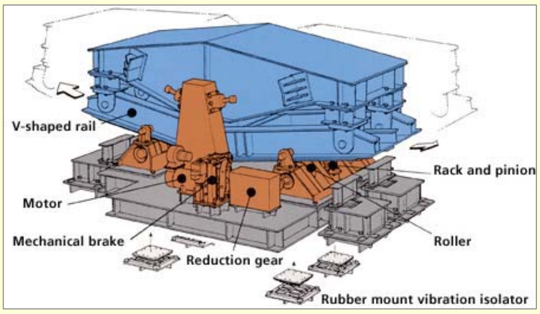

15

ULB

TRIGON pendulum device (Kajima corp. 1993)
Shinjuku Park Tower – Seismic Response Control

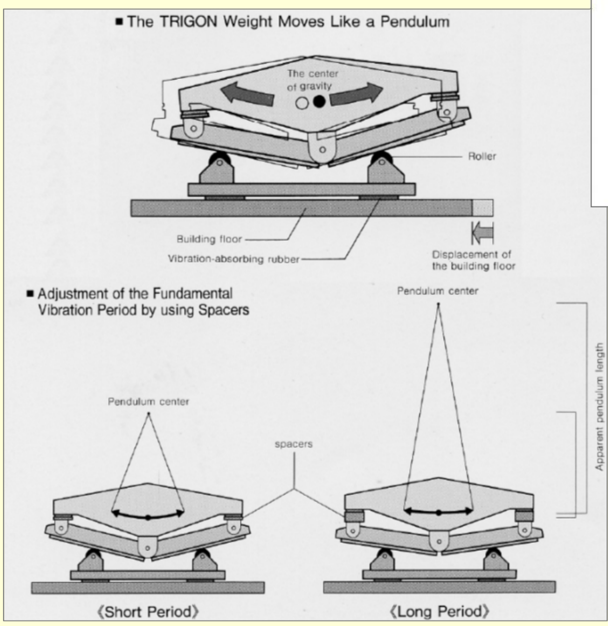

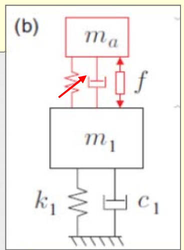

16

Suspension bridges

Golden Gate, San Francisco, 1280 m, 1937

Clifton Bridge Bristol (Brunel, 1864)

Largest span: Akashi bridge,
Kobe 1991 m, 1998

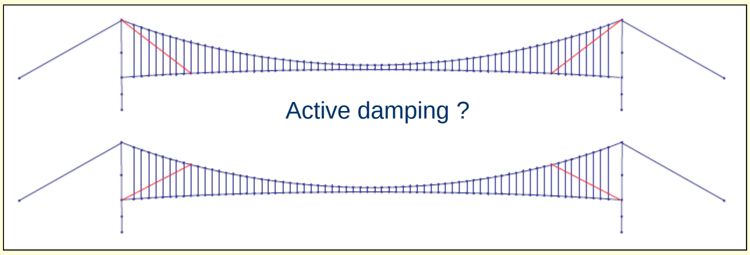

ULB

17

Decentralized active tendon control of cable-structures

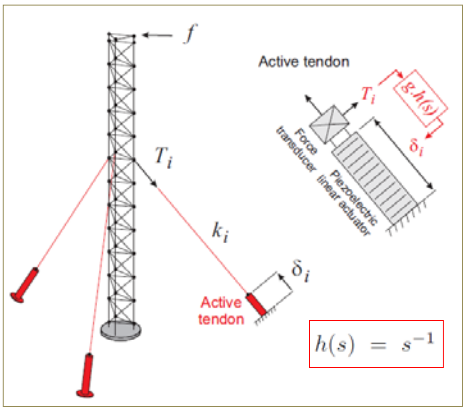

Maximum achievable damping:

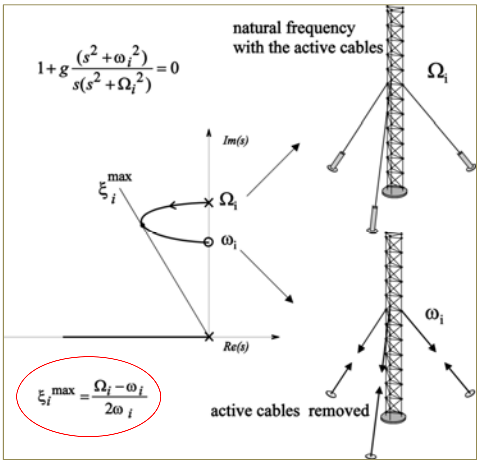

ULB

A.PREUMONT: *Vibration Control of Active Structures*, 3rd Edition, Springer 2011

18

Suspension bridge: Seriate footbridge

ULB

19

Mode N.	2D Numerical (Hz)	3D Numerical (Hz)	Experimental (Hz)	Numerical Mode Shape	Experimental Mode Shape
1^{st} B.	1.03	1.02	1.03 $\xi_1 = 2.77$ %	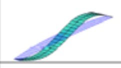	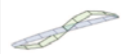
2^{nd} B.	1.39	1.48	1.48 $\xi_2 = 1.34$ %	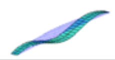	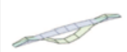
1^{st} T.	/	1.79	1.92	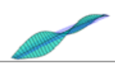	
2^{nd} T.	/	2.1	1.94	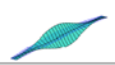	
3^{rd} B.	**2.22**	**2.20**	**2.17** $\xi_3 = 1.48$ %	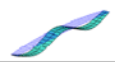	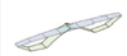
3^{rd} T.	/	2.65	2.75	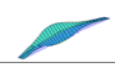	
4^{th} B.	**2.81**	**2.78**	**2.86** $\xi_4 = 1.50$ %	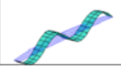	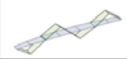

Table 1: Natural frequencies and mode shapes of the Seriate footbridge, comparison of the 3D model and 2D model with experiments [18]. The two critical modes are **3B** and **4B**.

Active tendon control with 4 steel cables of diameter 10 mm can bring up to 15% damping in the critical modes

ULB

20

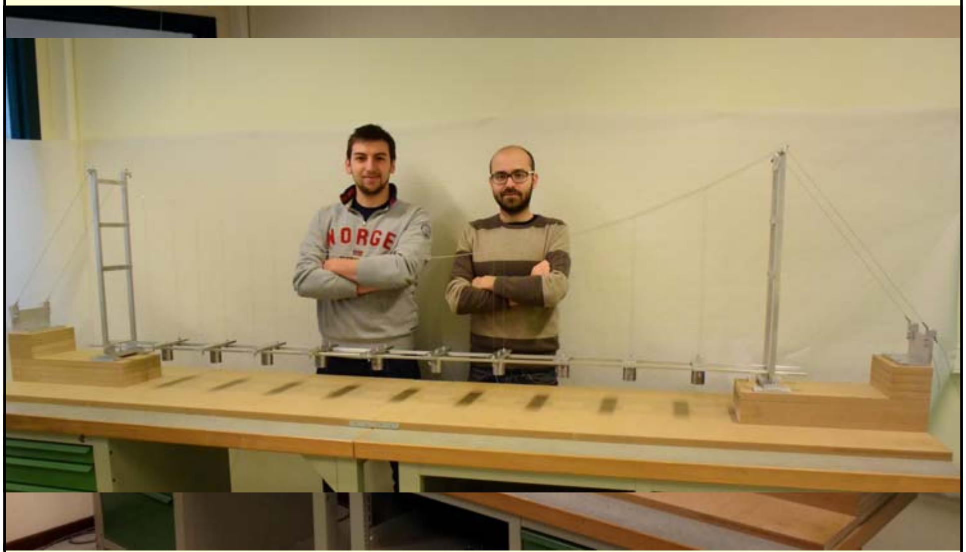

ULB

21

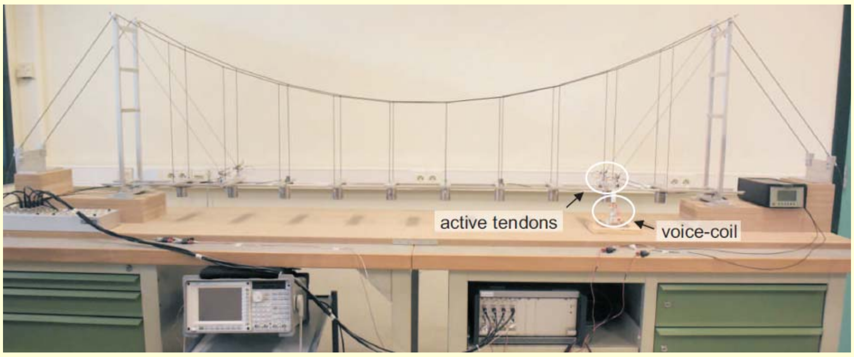

ULB

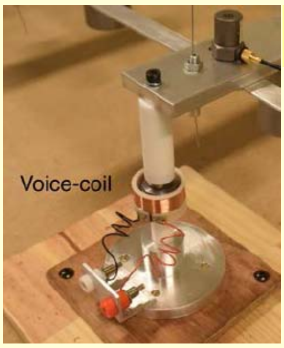

Mock-up with 4 active tendons

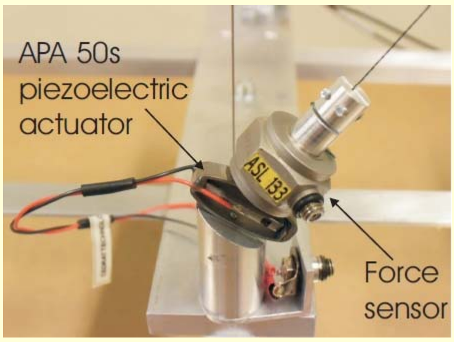

Decentralized control with Four independent loops
Reponse to disturbance z/f (FRF and cumulative RMS)

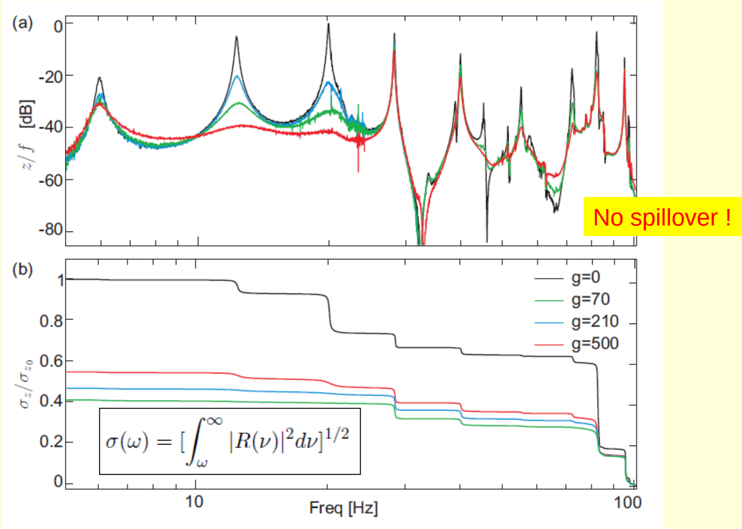

23

Multiple tower with active control bridges

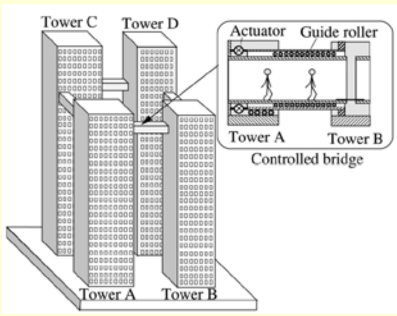

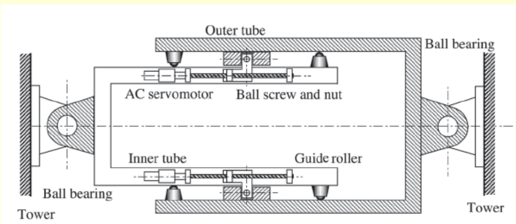

[K.Seto, 2008]

24

Multiple tower with active control Bridges - Laboratory Mock-up

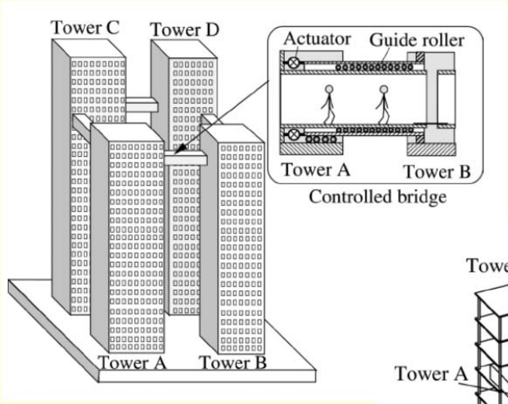

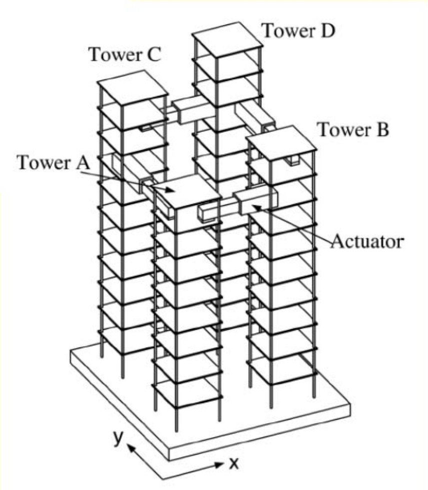

[K.Seto, 2008]

ULB

25

Shaking table tests

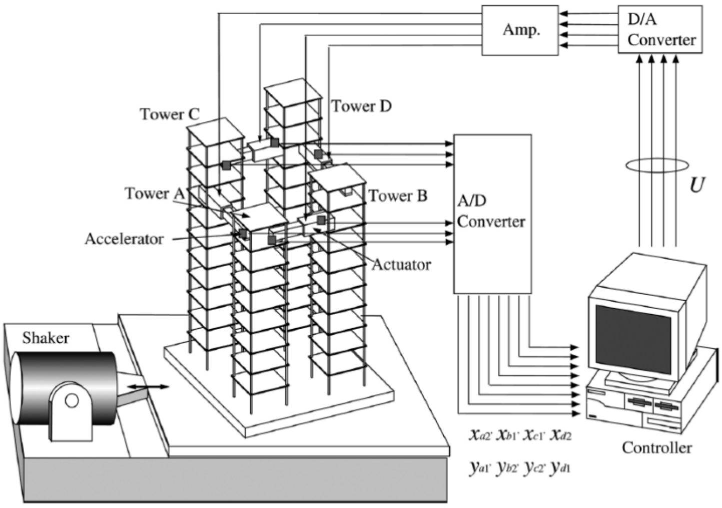

[K.Seto, 2008]

ULB

26

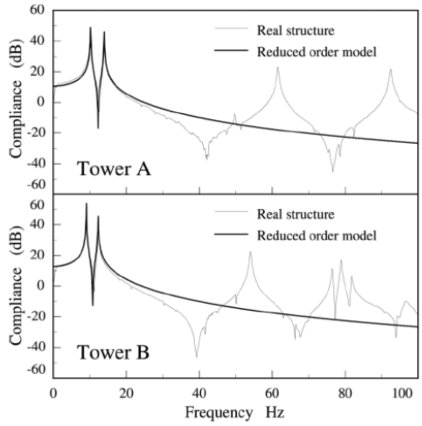

Comparison between the full model and a reduced 2 d.o;f. model

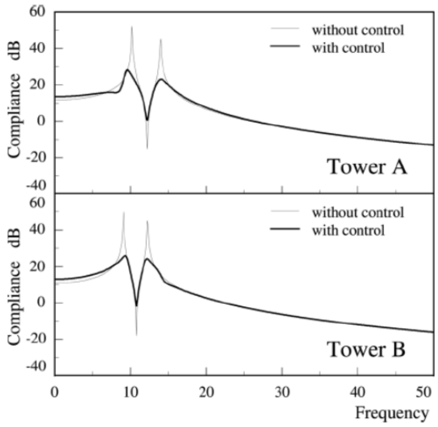

Frequency response with and without control

[K.Seto, 2008]

ULB

27

Seismic input

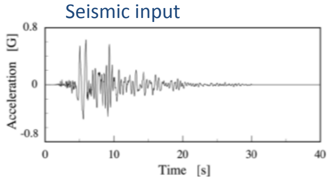

Simulated time response

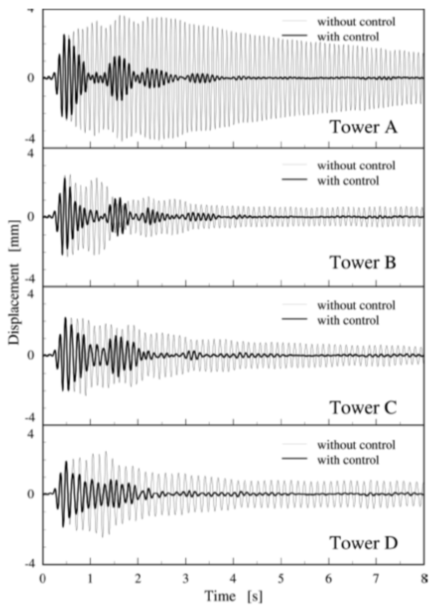

[K.Seto, 2008]

ULB

28

ULB

March 11, 2011 Earthquake (Fukushima)

Records with largest PGA : Tsukidate Station, Miyagi. Distance to epicenter : 125.9 Km, Distance to Fault 75Km

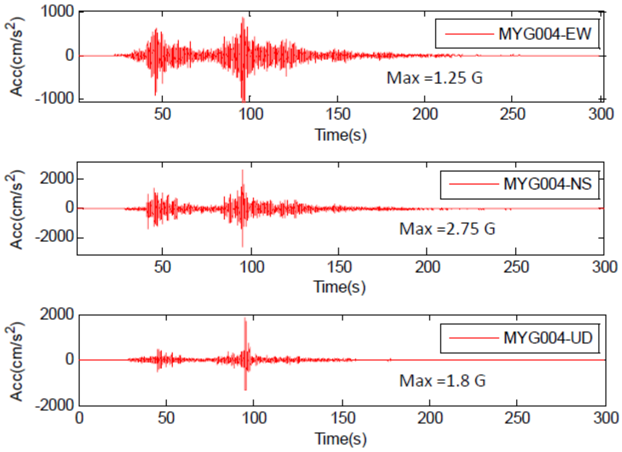

[Y.Fujino, 2011]

29

Triton Square building during Japon earthquake (3/2011)

ULB

30

ULB

Space interferometer

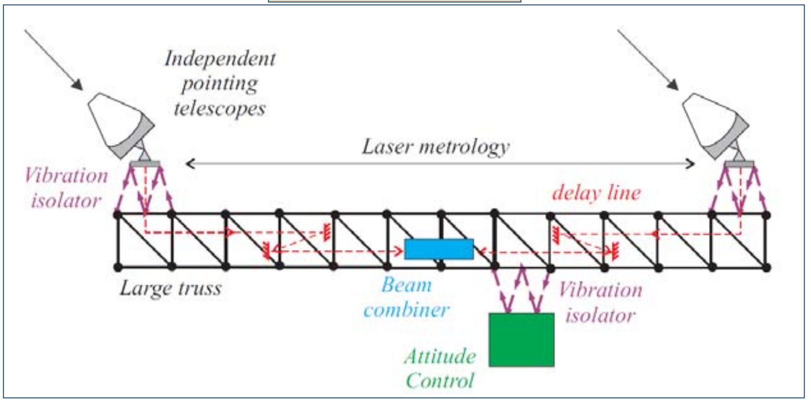

Optical Path Difference (OPD) accuracy: $\lambda/20$

- **Vibration isolation** from attitude control system & cryocooler
- **Damping** large truss structures
- **Co-phasing** telescopes (delay lines)
- **Wavefront Control (Adaptive Optics)**

31

James Webb Space Telescope (~ 2018)

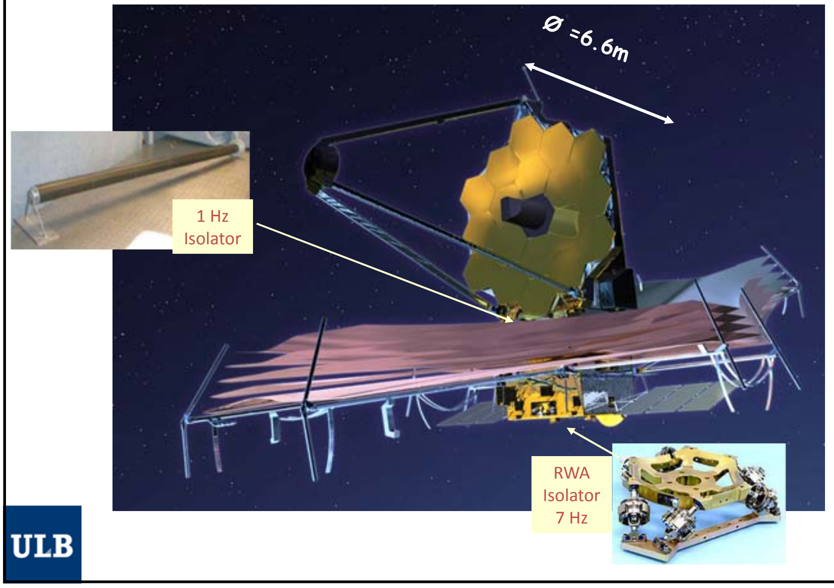

ULB

32

Effect of the isolator on the transmissibility of disturbances

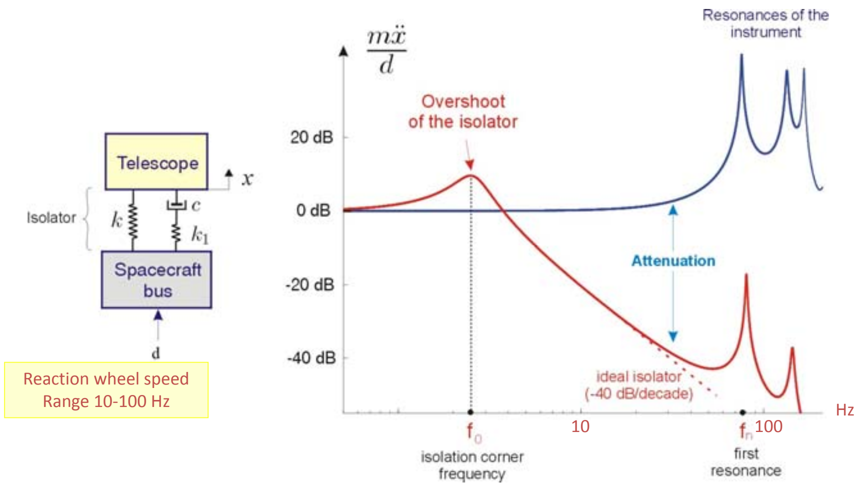

ULB

Various isolation concepts

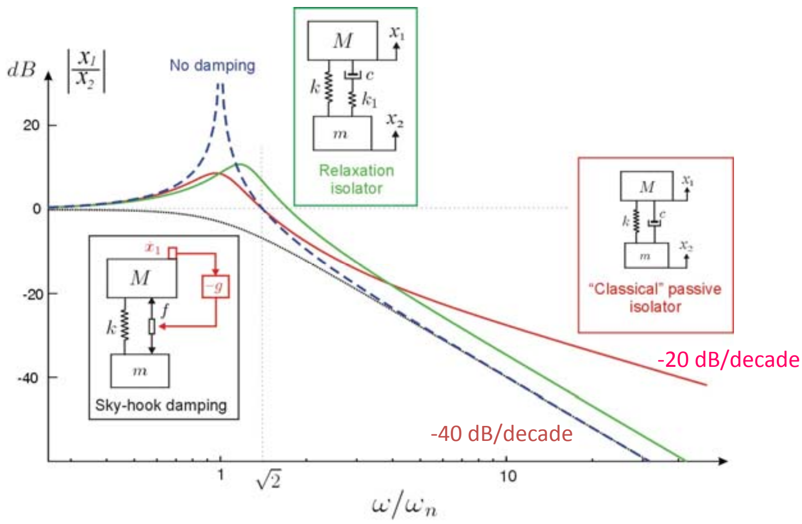

ULB

Sky-hook isolator (active)

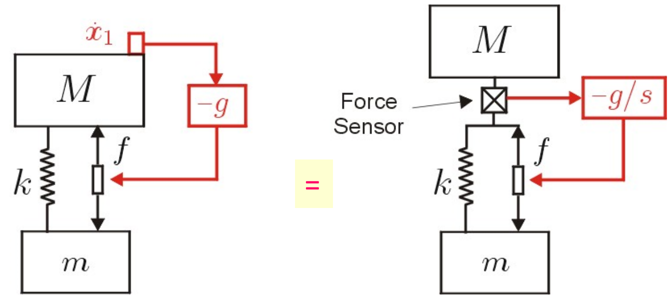

Velocity sensor

Force sensor

ULB

35

Robust implementation of the sky-hook isolator for **flexible** structures

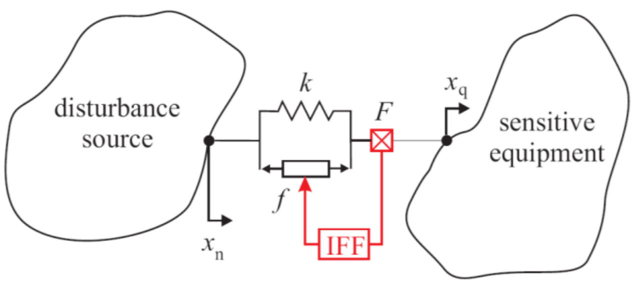

If two arbitrary flexible, undamped structures are connected with a single axis soft isolator with force feedback, the poles and zeros in the open-loop transfer function alternate on the imaginary axis.

ULB

36

Electromagnetic implementation of the **relaxation isolator**

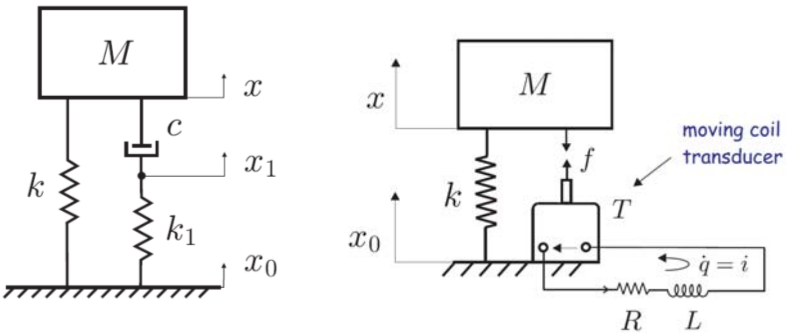

The two systems are equivalent provided that:

$$k_1 = \frac{T^2}{L} \qquad c = \frac{T^2}{R}$$

Electric components are often more flexible and
less temperature sensitive than elastomers

ULB

Six-axis isolator Zero-g experiment

ULB

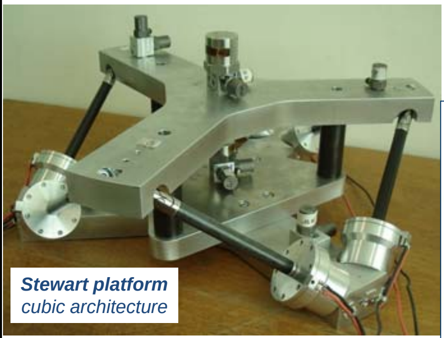

Stewart platform
cubic architecture

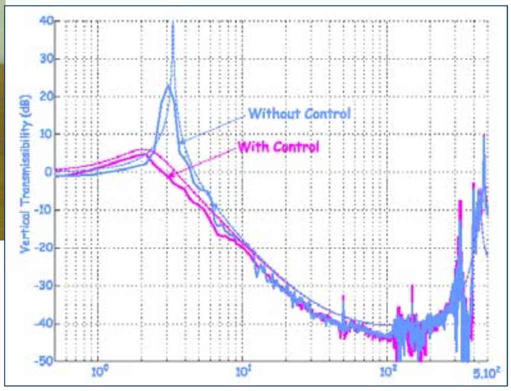

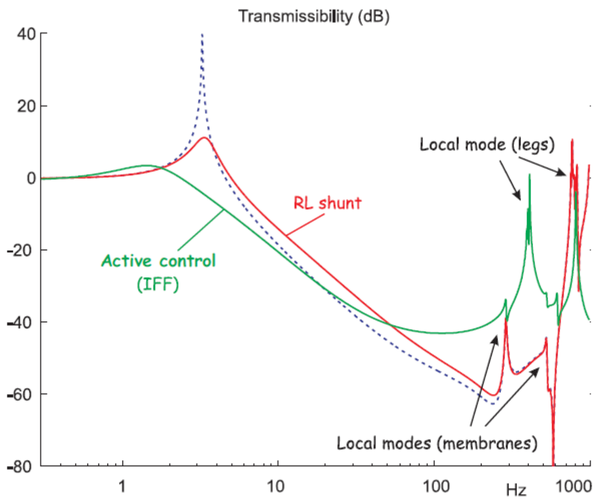

Fig. 8.26 Vertical transmissibility of a six-axis isolator: comparison of the Open-loop (dotted line), closed-loop (IFF) active isolator and passive relaxation isolator with a *RL* shunt (from de Marneffe et al.).

A brief history of earth-based telescopes

Galileo – 1610
discovered Jupiter's Moons
(refractive telescope)

Newton – 1668
reflective telescope
(removes the chromatic aberration)

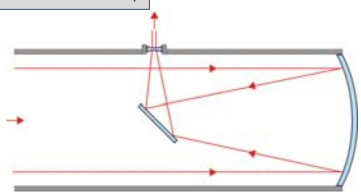


Herschel – 1781
discovered Uranus
with a telescope of D=17 cm

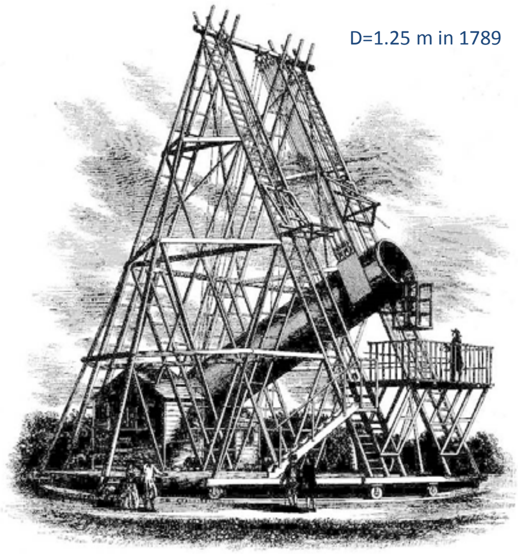
D=1.25 m in 1789

ULB

41


Mt Wilson-1917
D=2.5m

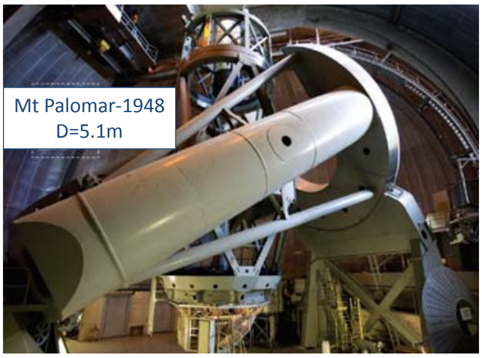
Mt Palomar-1948
D=5.1m


ESO-VLT-1998
D=8.2m, 150 actuators


Keck I & II (1993-1996)
D=10m, 36 segments

ULB

42

How big can it be ?

Size of optical telescopes vs. time

Log scale !

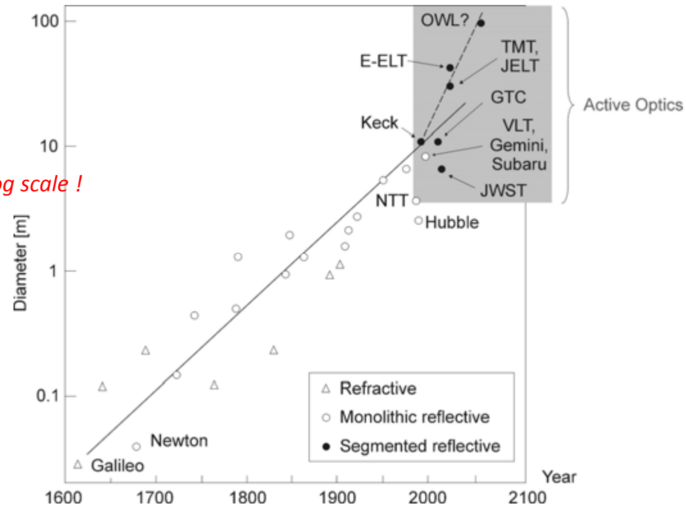

ULB

43

ULB

M1 of existing and future Optical telescopes

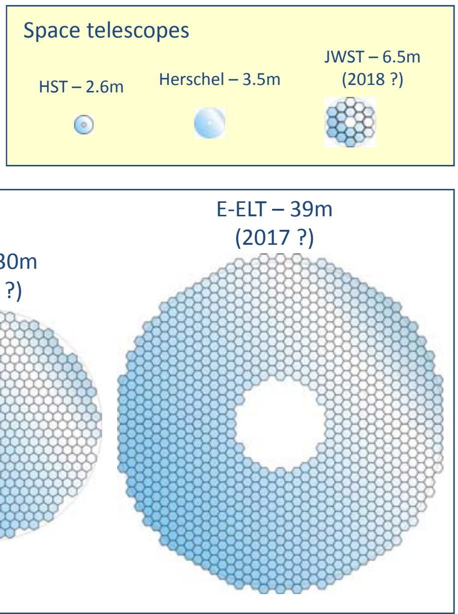

44

Principle of a reflective telescope

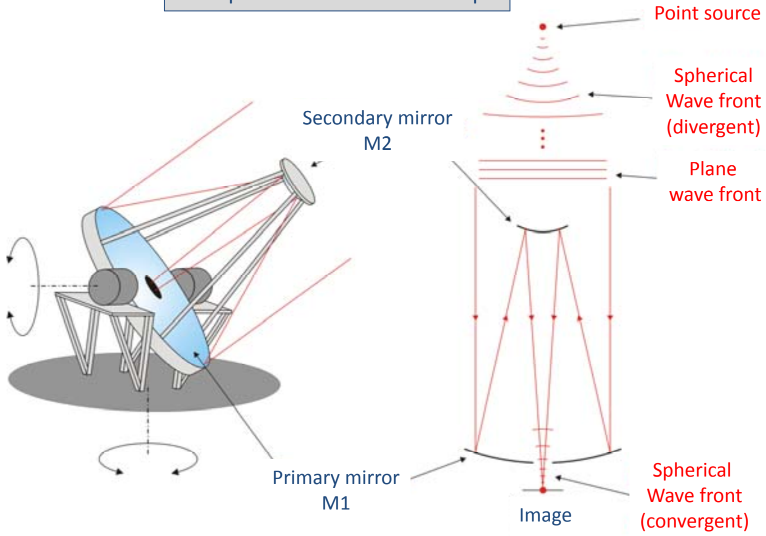

45

Optical aberrations

Motivation for larger M1:
Image quality

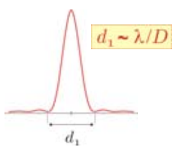

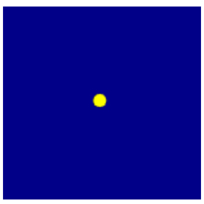

Point source

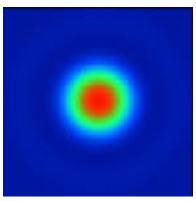

Diffraction

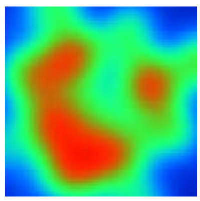

Aberration

Sources of aberrations (ground based telescopes):

Atmospheric turbulence: **Adaptive optics**

Gravity, wind excitation, thermal gradients: **Active optics**

If the RMS wave front error is **< λ/14**,
the telescope is considered as diffraction limited

ULB

46

Principle of Adaptive Optics

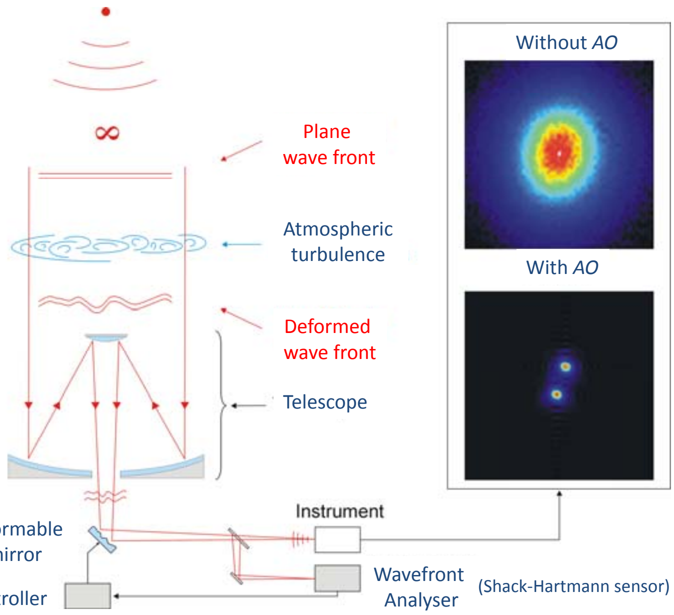

ULB

47

Piezoelectricity:

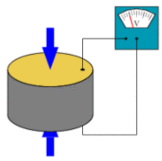

Bimorph actuation

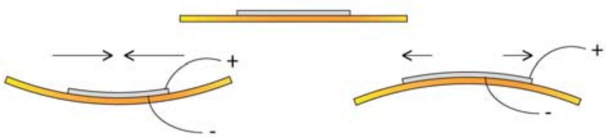

ULB

48

Bimorph Adaptive Optics Silicon Mirror

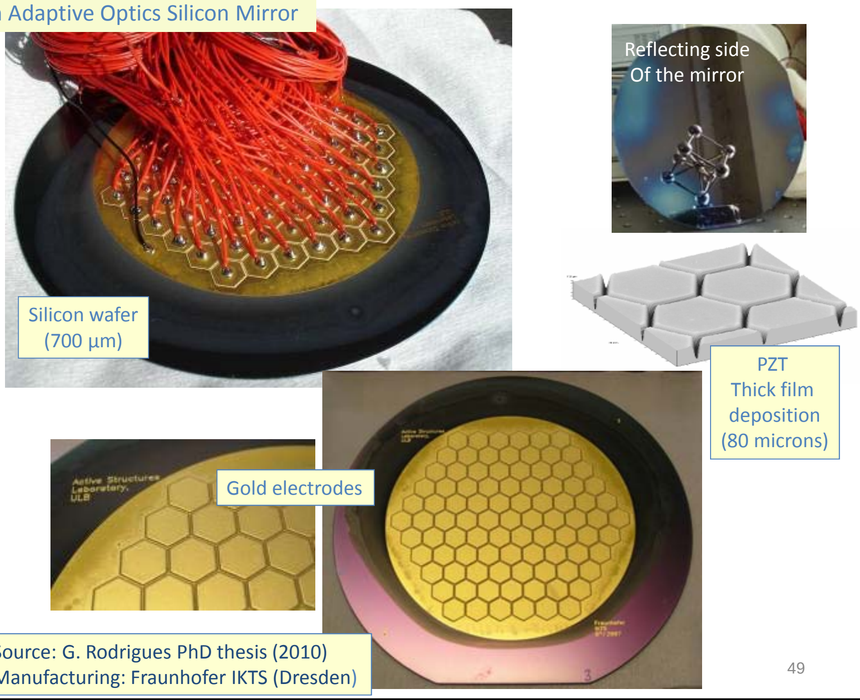

ULB

Source: G. Rodrigues PhD thesis (2010)
Manufacturing: Fraunhofer IKTS (Dresden)

49

ULB

Adaptive Optics Bench

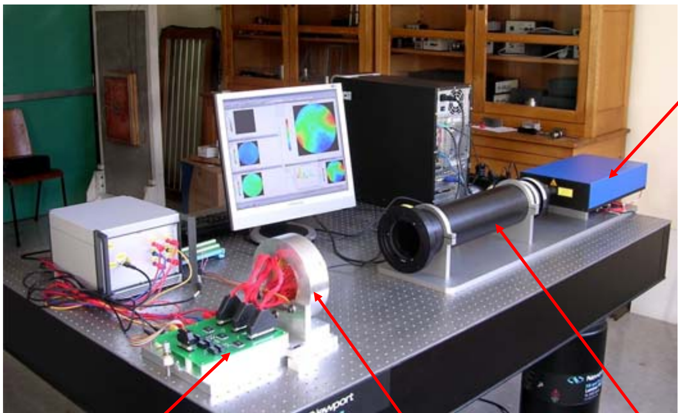

Collaboration with CSL

50

Closed-loop experiment

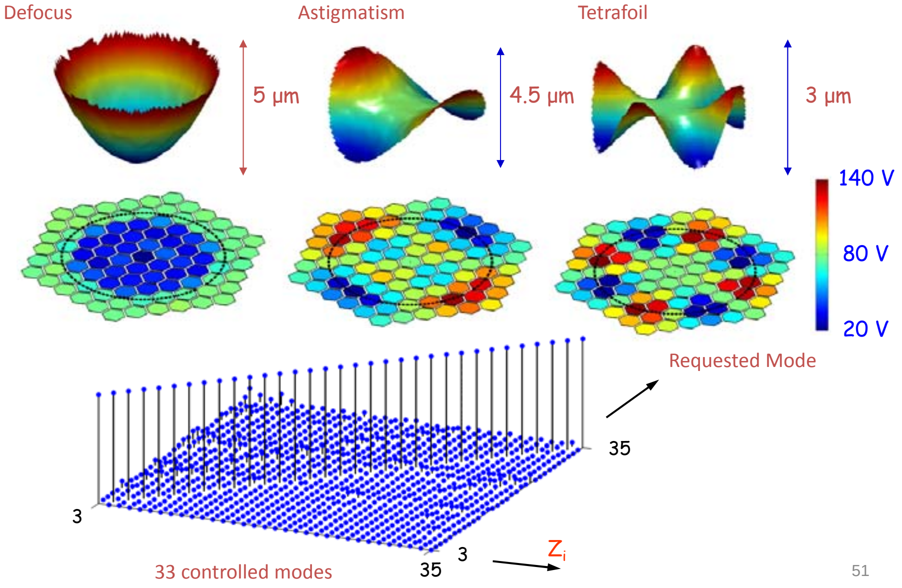

51

Adaptive Optics segmented mirror
Reference design (2013)

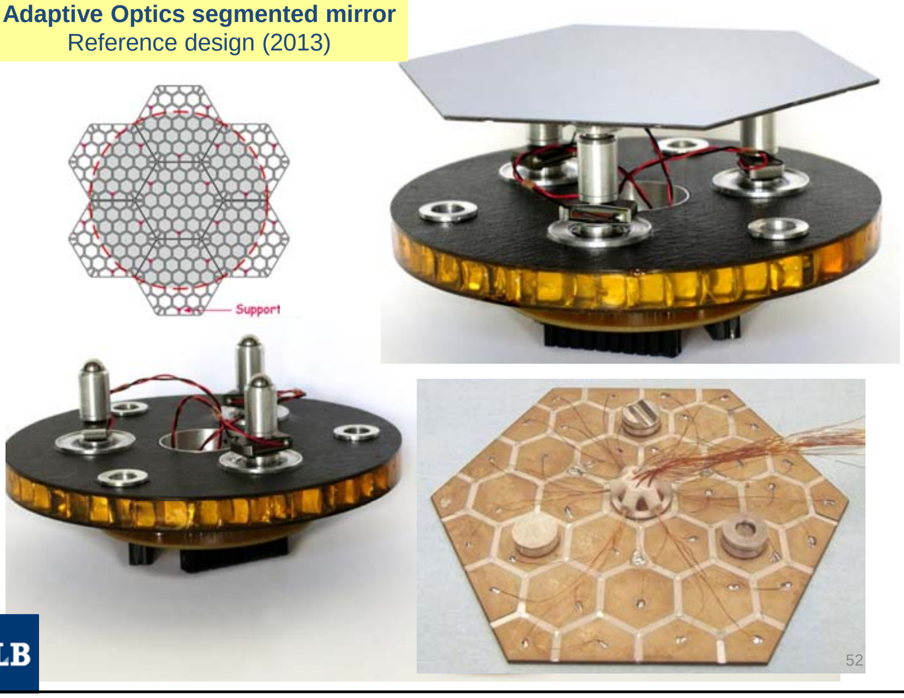

52

AO mirror with PZT actuation
Keystone electrode design (ESA-2015)

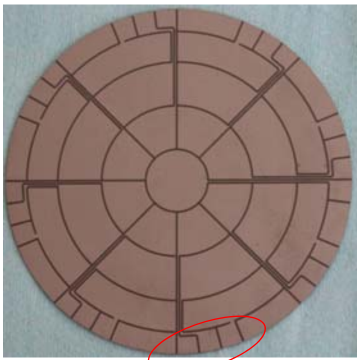

All electrical connections
Outside the pupil

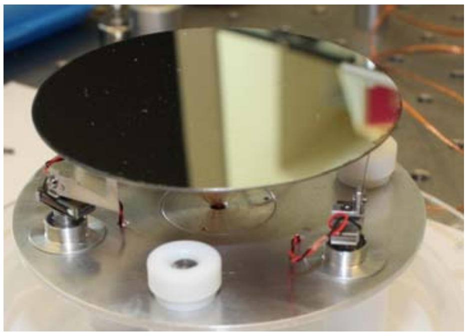

Rigid body actuators

ULB

Ultra-flat design (2016)

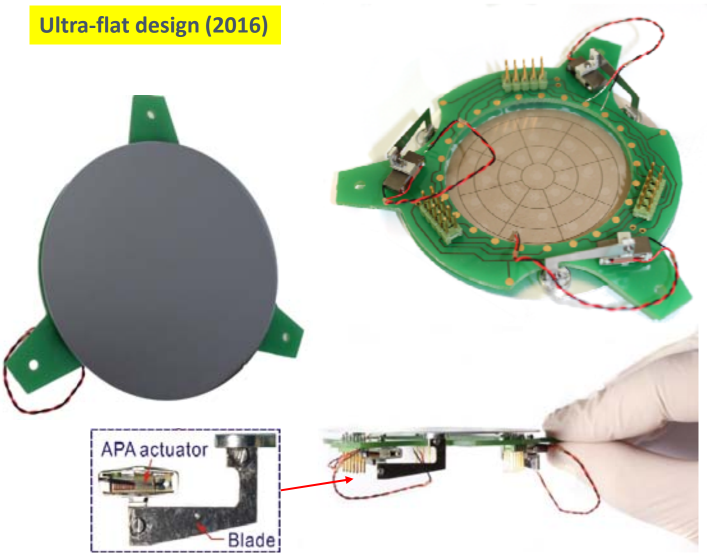

ULB

54

Comparison of numerical simulation and experiment for an incremental surface of 1µm of astigmatism. From top to bottom: surface figure, voltage map and residual error.

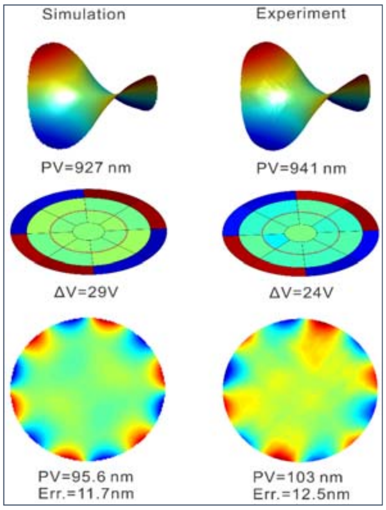

ULB

55

Active Optics

E-ELT primary mirror [ESO-2018?]

984 segments

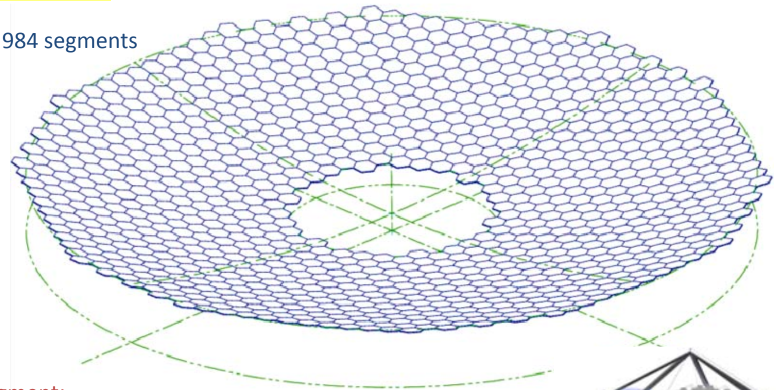

One segment:

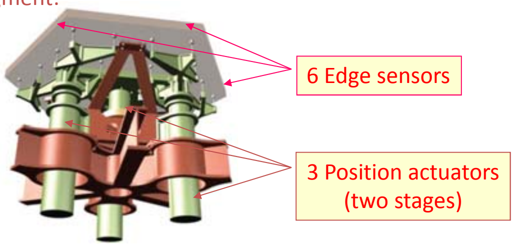

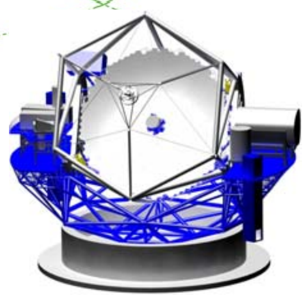

ULB

Effect of vibration on the Point Spread Function (PSF)

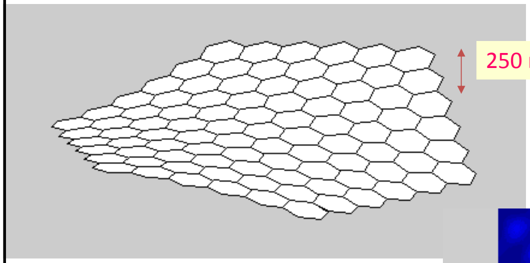

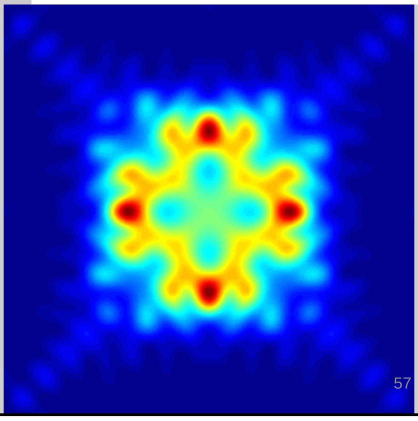

ULB

57

Truss-supported segmented mirror

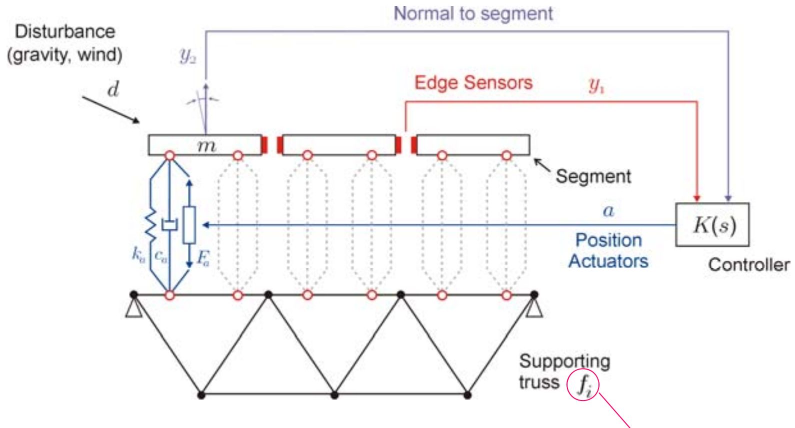

Quasi-static response: $y = J\,a$
(assuming the truss is infinitely rigid)

Dynamic uncertainty !

ULB

58

Static deflection under gravity

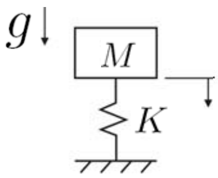

$$\Delta = \frac{Mg}{K} = \frac{g}{{\omega_1}^2}$$

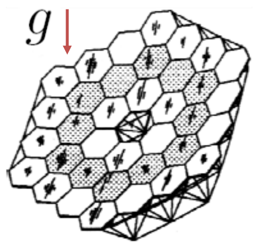

The static deflections under gravity scale according to

$$\Delta \propto f_1^{-2}$$

ULB

59

Truss supported segmented reflector
Scaling law for the first natural frequency

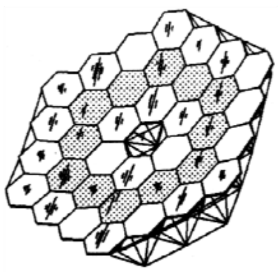

$$f_1 \sim \frac{0.852}{D}\left(\frac{h}{D}\right)\sqrt{\eta \cdot \frac{E}{\varrho}}$$

Specific modulus

$$\eta = \frac{\text{Truss Mass}}{\text{Truss Mass} + \text{Reflectror Mass}}$$

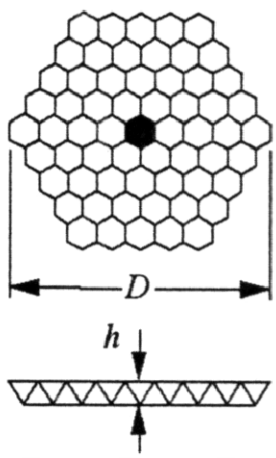

ULB (Source: Lake, Peterson & Mikulas, 2006)

60

Gravity compensation: ELT vs. VLT

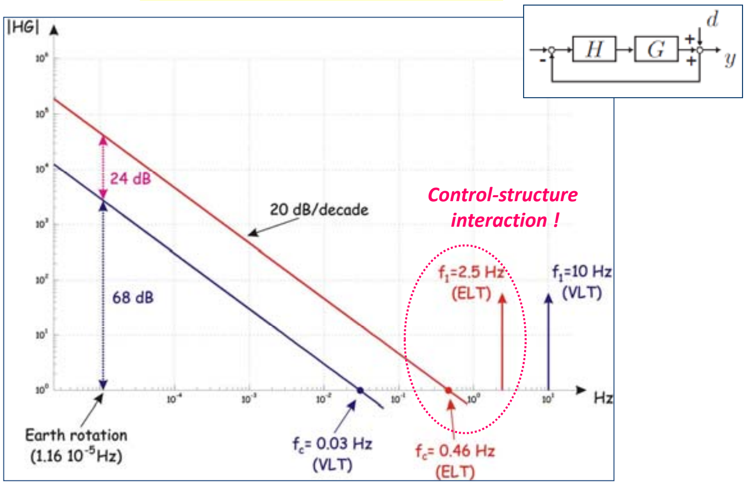

VLT: static deformations of 100 µm are reduced to 40 nm
ELT: static deformations increased by 16
Control bandwidth is increased from 0.03 Hz to 0.46 Hz

ULB

Control-structure interaction

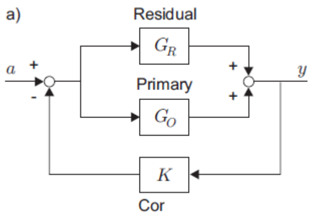

Sufficient condition for stability:

$$\bar{\sigma}[\mathbf{G}_0^{-1}\mathbf{G}_R(j\omega)] < \underline{\sigma}[I + (\mathbf{K}\mathbf{G}_0)^{-1}(j\omega)], \qquad \omega > 0$$

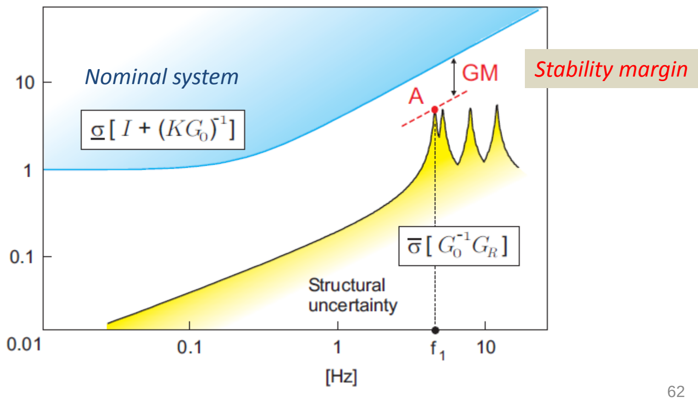

ULB

Conclusions:

- The **size** of civil engineering structures increases rapidly
- They become **more sensitive to vibrations** (wind, earthquake, traffic)
- This constitutes new opportunities for **active vibration control**
- The **actuator** is the most important component of the control system

Acknowledgements:

All my PhD students:
http://www.ulb.ac.be/scmero/publi.html

Our sponsors:
EU, ESA, ESF, FNRS-FRIA, Région Wallonne, FCT Portugal, Humboldt foundation…

Many colleagues scattered all over Europe and overseas,
from whom I have learned my job…

ULB

63